

Stochastic energetics of a Brownian motor and refrigerator driven by non-uniform temperature

Ronald Benjamin*

Institut für Theoretische Physik II, Universität Düsseldorf, D-40225 Düsseldorf, Germany.

(Dated: November 1, 2018)

The energetics of a Brownian heat engine and heat pump driven by position dependent temperature, known as the Büttiker-Landauer heat engine and heat pump, is investigated by numerical simulations of the inertial Langevin equation. We identify parameter values for optimal performance of the heat engine and heat pump. Our results qualitatively differ from approaches based on the overdamped model. The behavior of the heat engine and heat pump, in the linear response regime is examined under finite time conditions and we find that the efficiency is lower than that of an endoreversible engine working under the same condition. Finally, we investigate the role of different potential and temperature profiles to enhance the efficiency of the system. Our simulations show that optimizing the potential and temperature profile leads only to a marginal enhancement of the system performance due to the large entropy production via the Brownian particle's kinetic energy.

PACS numbers: 05.10.Gg, 05.40.Jc, 05.40.Ca, 05.60.Cd, 05.70.Ln

I. INTRODUCTION

It has been known since the works of Landauer [1], Van Kampen [2, 3] and Büttiker [4] that a Brownian particle in a periodic potential and subject to a spatially inhomogeneous and periodic temperature profile can move preferentially in one direction. In presence of a small external load it can also do work as a heat engine. Furthermore, according to Onsager symmetry the motor can also work as a refrigerator or heat pump, transferring heat from the cold to the hot bath in presence of an external power supply. This mechanism of directed transport and heat transport in presence of spatially non-uniform heat bath, is well known as the Büttiker-Landauer heat engine and heat pump. Along with the Feynman-Smoluchowsky ratchet and pawl heat engine [5, 6], this was one of the first examples of autonomous Brownian motors, which have subsequently been widely studied by many authors in recent years [7–14].

The BL heat engine/heat pump is an ideal system to investigate non-equilibrium thermodynamics of small scale systems where thermal fluctuations become important [15]. Thermodynamic quantities such as the work and heat which determine how effectively such microscopic engines perform their tasks and are also of great interest to the nanoscale industry desirous of building artificial Brownian motors. Sekimoto in 1997 formulated stochastic energetics [16], based on the Langevin equation, to quantify the heat flow and efficiency of such Brownian engines.

Several authors have investigated the energetics of the Büttiker-Landauer heat engine and heat pump using Sekimoto's formulation. It was shown using overdamped models (mass of the Brownian particle $M = 0$) [10, 11, 17] based on the Fokker-Planck equation as

well as based on other phenomenological approaches [12], that the BL heat engine can reach Carnot efficiency and the BL heat pump can attain the corresponding Carnot coefficient of performance. However, Derényi-Astumian [8] and Hondou-Sekimoto [9] later argued that Carnot efficiency is unattainable due to the irreversible heat flow via kinetic energy from the hot to the cold bath whenever the Brownian particle crosses a temperature boundary. They made phenomenological predictions regarding the failure of overdamped models in predicting this heat transfer and argued that the heat flow via kinetic energy diverges in the overdamped limit ($M \rightarrow 0$).

In a recent work [14], stochastic energetics of the Büttiker-Landauer heat engine and heat pump was investigated by a direct comparison of numerical solution of the inertial Langevin equation with molecular dynamics simulations. Good agreement between the two approaches confirmed Sekimoto's stochastic energetics as well as the predictions of Derényi-Astumian [8] and Hondou-Sekimoto [9] and showed that the overdamped model ($M = 0$) is not equivalent to the overdamped limit ($M \rightarrow 0$). In fact one should take into account the inertial mass of the Brownian particle and then go to the overdamped limit. At the quasistatic limit corresponding to zero average motor velocity, where overdamped models predict Carnot efficiency, the true efficiency is actually zero because even if heat flow via potential vanishes, the irreversible heat flow via kinetic energy does not vanish. This irreversible heat also dominates the heat flow via the potential and greatly reduces the efficiency of the heat engine and the coefficient of performance of the heat pump.

Carnot efficiency, if attainable, is reached only in the quasistatic limit, when the operating time of the engine is infinite and the power output is thus zero. Since a real heat engine must produce power in a finite time, it is more appropriate to analyse its efficiency under the condition of maximum power. In a recent work, Van den Broeck [18] has shown that in the linear response

*Electronic address: ronbenin@yahoo.com

regime, the efficiency at maximum power of a Brownian engine reaches the efficiency of an endoreversible engine when it operates at maximum power, namely the Curzon-Ahlborn efficiency [19]. Corresponding to the efficiency at maximum power, some authors have studied the equivalent quantity for the heat pump using linear irreversible thermodynamics [20]. Analytical expressions for the efficiency at maximum power [18, 21–23] and the corresponding quantity for a heat pump have been derived but the validity of these expressions have not been confirmed for the BL heat engine/heat pump for a finite mass of the Brownian particle.

The efficiency at maximum power of the BL heat engine has been studied using overdamped models [11], and the authors showed that it is close to the Curzon-Ahlborn efficiency. Gomez-Marin and Sancho [24] studied a certain model of the BL heat engine/heat pump based on the overdamped Fokker-Planck equation and concluded that efficiency at maximum power in the linear response regime is equal to Curzon-Ahlborn efficiency. However, as was pointed out by the them, a proper analysis of the thermodynamics of the BL heat engine in the linear response regime can only be made by considering the inertial term since irreversible heat flow via kinetic energy plays an important role in its energetics.

While the dominant contribution to the heat flow comes from the kinetic energy contribution, many authors ignore the kinetic energy contribution and discuss ways to enhance efficiency of the BL heat engine based on an overdamped approach. Some papers have reported a very high efficiency for the BL heat engine, of the same order as the Carnot efficiency, in certain parameter regimes. These works discuss various strategies to enhance the efficiency of the BL heat engine by modifying the potential and temperature profiles. However, such approaches towards designing a more efficient heat engine have not been tested by considering mass of the Brownian particle and thus the heat flow via kinetic energy.

Since, kinetic energy plays such a crucial role in presence of spatially inhomogeneous temperature, a more complete description of the thermodynamics of the BL heat engine requires taking into consideration mass of the Brownian particle explicitly. As kinetic energy contribution dominates over the heat transfer via the potential, one should first attempt to reduce the kinetic energy contribution and then discuss other ways to enhance the efficiency. While some works have tried to include the irreversible heat flow via kinetic energy in a phenomenological manner in their theoretical calculations [25–27], a direct quantification of this irreversible heat is not to be found in the literature apart from the simulation study of Ref. [14]. However, in Ref. [14], only one model of the BL heat engine was investigated and there was no discussion on possible ways to enhance the efficiency of the heat engine. Moreover, energetics of the Brownian heat pump or refrigerator based on a spatially non-uniform temperature was not considered.

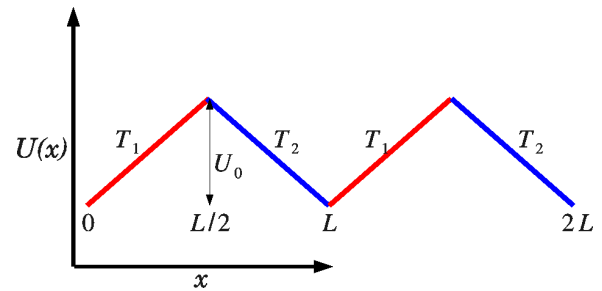


FIG. 1: (Color online) Two rectangular reservoirs at temperatures T_1 and T_2 are alternately connected. Brownian particles are subjected to a piece-wise linear potential.

In the present work, we attempt to fill an important gap in the study on the thermodynamics of the BL heat engine by explicitly taking into account the mass of the Brownian particle. As we show in the next sections, our results qualitatively differ with previous studies on the efficiency optimization of the BL heat engine based on overdamped approaches. We will investigate the energetics of the BL heat engine and heat pump by extensive numerical simulations of the Langevin equation. First, we numerically explore the optimal conditions for performance of the BL engine. Then we will discuss the operation of the system in the linear response regime and test the validity of the expressions for the efficiency and coefficient of power under finite time conditions. Finally we consider different temperature and potential profiles to diminish the kinetic energy contribution and enhance the performance of the heat engine and heat pump.

The paper has been organized as follows: in the next section we introduce the basic model, as studied in a previous work [14], and the methods used to investigate the energetics of the BL heat engine and heat pump. In sections III and IV, we discuss the efficiency of the BL heat engine and heat pump respectively based on the basic model. Section V discusses the efficiency and coefficient of performance in the linear response regime. In section VI, we study the effect of different potential and temperature profiles on the heat engine efficiency and heat pump coefficient of performance. Finally, we end with a conclusion.

Throughout this paper, we use the terms motor and heat engine interchangeable to mean the same thing i.e. a Brownian motor doing work against an external load. Similarly the terms heat pump and refrigerator mean the same thing.

II. BASIC MODEL AND METHODS

We consider a chain of two-dimensional cells attached to each other along the x direction (see Fig. 1). Each cell is $L/2$ long and filled with heat bath particles. The cells are thermally isolated from each other and at thermal equilibrium with a temperature independent from

the neighbouring cells. Brownian particles of mass M are placed in the cells and, unlike the heat bath particles, can move through the cell walls. They are also subjected to a periodic piece-wise linear potential $U(x)$ with a period L in the x direction:

$$U(x) = \begin{cases} -\frac{2U_0}{L}x & \text{for } -\frac{L}{2} < x \leq 0, \\ \frac{2U_0}{L}x & \text{for } 0 < x \leq \frac{L}{2}, \end{cases} \quad (1)$$

where U_0 is the potential height. In addition to the periodic potential, a constant external force F is exerted on the Brownian particles. Instead of infinitely long chains we consider only two cells with a periodic boundary condition: cell 1 with temperature T_1 for $-L/2 < x \leq 0$ and cell 2 with T_2 for $0 < x \leq L/2$.

The motion of the Brownian particle in the x direction can be investigated by the one-dimensional Langevin equation:

$$\begin{aligned} \dot{x} &= v, \\ M\dot{v} &= -\gamma(x)v - U'(x) + F + \sqrt{2\gamma(x)T(x)}\xi(t), \end{aligned} \quad (2)$$

where x and v are the position and velocity of the Brownian particle and $\xi(t)$ is a standard Gaussian white noise:

$$\langle \xi(t) \rangle = 0, \quad \langle \xi(t)\xi(s) \rangle = \delta(t-s). \quad (3)$$

The piecewise constant temperature is given by:

$$T(x) = \begin{cases} T_1 & \text{for } -\frac{L}{2} < x \leq 0, \\ T_2 & \text{for } 0 < x \leq \frac{L}{2}. \end{cases} \quad (4)$$

Temperature is measured in energy unit ($k_B = 1$). Here, and later on, an overdot refers to derivative taken with respect to time and a prime means derivative taken with respect to space. Assuming that Einstein's relation, namely, $D(x) = T(x)/\gamma(x)$ holds locally, the friction coefficient also depends on the position in the same way as the temperature through the relation

$$\gamma(x) = \rho\sigma_B\sqrt{2\pi T(x)m}, \quad (5)$$

where, ρ , m and σ_B refer to the number density of heat bath particles in a cell ($\rho = 0.01$ in all our simulations), the mass of a bath particle and the diameter of the Brownian particle, respectively. The above analytical expression for $\gamma(x)$ holds for an ideal gas [28]. Since, in our previous work [14], Langevin equation results were compared with hard-disk simulations of a Knudsen gas, we use the same dependence of the friction coefficient on the temperature for our Langevin simulation. The length of the simulation box was $L = 500$. We used the Heun algorithm [29] to numerically solve Eq. 2 with a time-step of $\tau = 0.001$ ($M/\gamma > 1.0$ corresponding to the underdamped regime) or 0.0001 ($M/\gamma \leq 1.0$ corresponding to the overdamped regime). For ease of numerical implementation all of our simulations were done in reduced units [6].

In order to investigate the thermodynamic properties, we use stochastic energetics formulated by Sekimoto [16, 30, 31]. The heat flux from the gas particles in the i -th cell to the Brownian particles is defined as,

$$\dot{Q}_i = \left\langle \left(-\gamma_i \dot{x} + \sqrt{2\gamma_i T_i} \xi(t) \right) \dot{x} \right\rangle_i, \quad (6)$$

where, $\langle \dots \rangle_i$ indicates ensemble average taken while the Brownian particles are located in the i -th cell. Using the Langevin equation (2), we obtain the total heat flux as a sum of three terms:

$$\begin{aligned} \dot{Q}_i &= \frac{M}{2} \frac{d}{dt} \langle \dot{x}^2 \rangle_i + \langle U'(x) \dot{x} \rangle_i - F \langle \dot{x} \rangle_i \\ &= \dot{Q}_i^{\text{KE}} + \dot{Q}_i^{\text{PE}} + \dot{Q}_i^{\text{J}} \end{aligned} \quad (7)$$

where the first two terms on the rhs are the kinetic energy and potential energy contribution to the heat flux, respectively, and the last term is the Joule heat. Rate of work done on a Brownian particle (or the power), by the external force F in each cell is given by,

$$\dot{W}_i = F \langle \dot{x} \rangle_i. \quad (8)$$

and the total power is given by,

$$\dot{W} = F(\langle \dot{x} \rangle_1 + \langle \dot{x} \rangle_2) = F \langle \dot{x} \rangle \quad (9)$$

where, $\langle \dot{x} \rangle_1 = \langle \dot{x} \rangle_2 = \langle \dot{x} \rangle / 2$, since width of both cells are the same and, $\langle \dot{x} \rangle = \langle v \rangle$ is the net particle current. Since, \dot{W} represents the total rate of work done on the Brownian particle, the power output in case of a heat engine is $-\dot{W}$. When the system functions as a heat engine in presence of an external load ($F < 0$), the net velocity $v > 0$ and therefore the power output $-\dot{W} > 0$. In case of a heat pump, \dot{W} represents the supplied power or the power input.

In the steady state, the net energy flux to the Brownian particles will vanish, and thus the energy gained by the Brownian particles in cell 1 will be cancelled by the energy loss in cell 2. Therefore, heat flux from cell 1 to cell 2 via the Brownian particles is defined as

$$\begin{aligned} \dot{Q}_{1 \rightarrow 2} &= \dot{Q}_1 + \dot{W}_1 = \dot{Q}_1^{\text{KE}} + \dot{Q}_1^{\text{PE}} \\ &= -\dot{Q}_2 - \dot{W}_2 = -\dot{Q}_2^{\text{KE}} - \dot{Q}_2^{\text{PE}}. \end{aligned} \quad (10)$$

The above equation represents the first law of thermodynamics as applied to the BL heat engine, which can also be written as,

$$\dot{Q}_1 = -\dot{Q}_2 - \dot{W} \quad (11)$$

which tells us that part of the net heat extracted from the hot bath is used by the Brownian particle to perform work against the external load and the rest is dissipated as heat to the cold bath.

A Brownian heat engine is in a non-equilibrium state and according to the second law of thermodynamics, the net entropy production during the working of the motor

must be positive. For the BL motor described above, which operates under the influence of two heat baths at different temperatures, the entropy production according to the second law is [15],

$$\dot{S} = -\frac{\dot{Q}_1}{T_1} - \frac{\dot{Q}_2}{T_2} \geq 0 \quad (12)$$

The thermodynamic efficiency of the BL heat engine, is defined as

$$\eta = \frac{-\dot{W}}{\dot{Q}_1} \quad (13)$$

and using the first and second laws, can be written as,

$$\eta = \eta_c - \frac{\dot{S}}{\dot{Q}_1} T_1 \quad (14)$$

where, $\eta_c = 1 - T_2/T_1$ is the Carnot efficiency.

Similar to the efficiency of the heat engine, one can define the coefficient of performance as, ε , defined as,

$$\varepsilon = \frac{\dot{Q}_2}{\dot{W}}, \quad (15)$$

and using the first and second laws of thermodynamics, Eq. 15 can be written as,

$$\varepsilon = \frac{\varepsilon_c \dot{Q}_2}{\varepsilon_c T_1 \dot{S} + \dot{Q}_2} \quad (16)$$

where, $\varepsilon_c = T_2/(T_1 - T_2)$.

The respective Carnot limits for the heat engine efficiency and heat pump coefficient of performance are attainable only if the entropy production \dot{S} vanishes, such that the engine works in a reversible way. However, Carnot efficiency, if attainable, is possible only under a quasistatic condition when the engine does no work or the heat pump transfer no heat. For the BL heat engine/heat pump however, there is production of entropy even in the quasistatic limit and hence it never attains the Carnot efficiency [14]. On the other hand, any finite power output or heat transfer will always be accompanied by entropy production which limits the efficiency/coefficient of performance of the heat engine/heat pump and part of the effort in this paper is devoted to finding out possible models with minimal entropy production leading to a higher efficiency, though without much success, as we will find out in the latter sections.

III. EFFICIENCY OF THE HEAT ENGINE

When two cells have different temperatures ($T_1 > T_2$), Brownian particles in the hotter cell can reach the higher-potential energy region more often than those in the low-temperature cell. As a result, the Brownian particles tend to move from the hot to the cold cell over the potential barrier, resulting in a net current in the positive

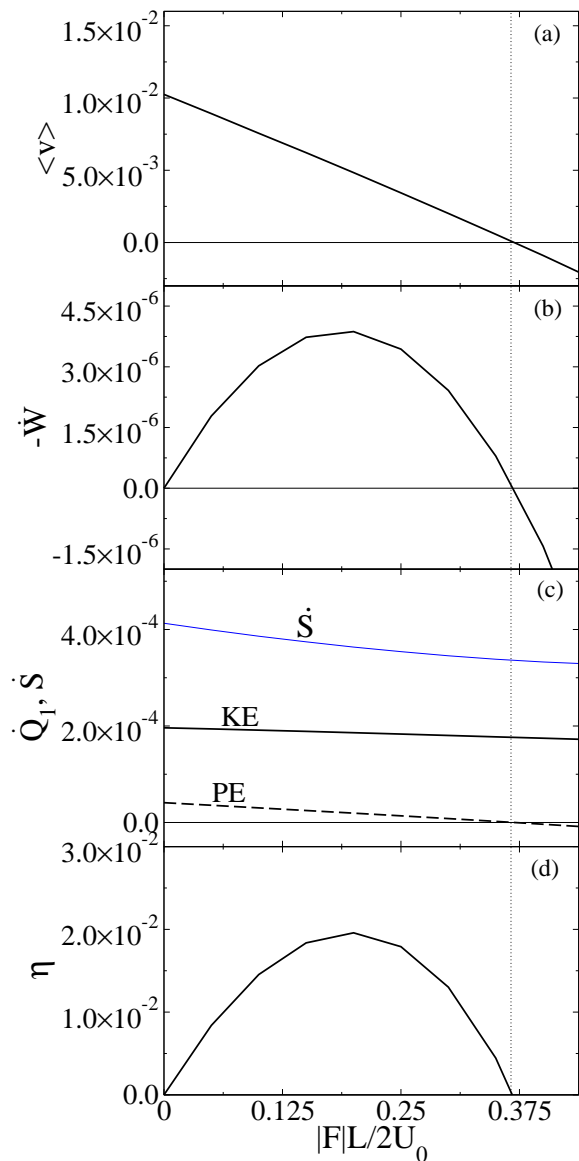


FIG. 2: (a) Average velocity $\langle v \rangle$, (b) power $-\dot{W}$, (c) \dot{Q}_1^{KE} , \dot{Q}_1^{PE} and \dot{S} , and (d) efficiency of the heat engine as a function of $|F|L/2U_0$. In (a), (b) and, (c), the thin horizontal solid line represents $y = 0$. The vertical line coincides with the stall load F_{stall} , where the motor velocity, work output and efficiency go to zero. The parameter values are $T_1 = 0.7$, $T_2 = 0.3$, $\sigma_B = 5$ and $M/m = 5$. The Carnot efficiency $\eta_c = 0.57$.

direction even in the absence of an external force ($F = 0$). In the presence of an external load ($F < 0$), the Brownian particles can do work against it behaving as a motor.

In Fig. 2, we plot the velocity, the power ($-\dot{W}$), various components of the heat flow out of cell 1 at temperature T_1 , the entropy production \dot{S} and efficiency as a function of the external load. As the external load impedes the motion of the Brownian particles, the velocity decreases and vanishes at the stall load F_{stall} . When $F = 0$, the

average velocity of the Brownian particles is not zero, but the work is zero. At the stall load, since the motor velocity goes to zero, the power output again vanishes. At a certain value of F , between 0 and F_{stall} , close to $F_{\text{stall}}/2$, the power output reaches a maximum i.e., the Brownian heat engine delivers maximum power. Now we come to the heat transfer. When the Brownian particle crosses one period to the right it extracts potential energy U_0 from the higher-temperature cell at the rate $(2U_0/L)\langle\dot{x}\rangle_1$ and dissipates the same amount of potential energy to the cold cell. This heat flow via potential decreases with the load as the velocity decreases and ultimately vanishes at F_{stall} . At the quasistatic limit of zero velocity, this heat transfer via potential energy is reversible.

On the other hand, Fig. 2 shows that the heat flow via kinetic energy varies slowly with the load and is positive even in the quasistatic limit, showing that a net heat flows from the hot to the cold reservoir even when the heat engine does not deliver any work. As explained in a previous work [14], when the Brownian particle crosses a temperature boundary its kinetic energy thermalizes to the new temperature thereby dissipating heat. Even when the motor velocity is zero at the stall load F_{stall} , the Brownian particles are still crossing the temperature boundary back and forth. Therefore, this heat continues to flow at the stall load. Since the heat flows always from the hot cell to the cold cell, independent of the direction of the Brownian particle's movement, it is irreversible heat. As Fig. 2 shows, at the stall load, the heat flow via potential is zero but the kinetic energy contribution is still positive leading to a non-zero entropy production.

The presence of this entropy producing irreversible heat carried by the kinetic energy of the Brownian particle, makes it impossible for the BL heat engine to reach Carnot efficiency, $\eta_c = 1 - T_1/T_2$. In fact, Fig. 2 shows that the efficiency is an order of magnitude lower than η_c and diminishes to zero at the quasistatic limit.

Beyond the stall load, the motor reverses its velocity and moves in the direction of the external load. In this situation work is done on the Brownian particle and hence the power output is negative and so is the heat flow via potential.

Figure 3 shows the power, heat flow via kinetic energy, and heat engine efficiency as a function of the temperature difference between the two cells. Overdamped models [11], which ignore the kinetic energy contribution, predict that the efficiency increases with ΔT and then saturates. However, when we take inertia into account, its a different story. At smaller ΔT , the power output is low leading to a low efficiency while at large ΔT , the heat flow via kinetic energy is large, again reducing the efficiency. While the power output saturates with increasing temperature difference between the cells, the entropy production and heat flow via kinetic energy monotonically increase with ΔT . There is an optimum ΔT at which the efficiency is maximum, but it is far lower than the Carnot efficiency. We also carried out simula-

tions where the friction coefficients in both the hot and cold baths were taken to be the same, but observed the same dependence of the thermodynamic quantities on the temperature difference between the cells.

It was shown in a previous work [14] that \dot{Q}^{KE} diverges as $M^{-1/2}$ in the overdamped limit ($M \rightarrow 0$). This can be understood as follows: the Brownian particle thermalizes over a length scale $l_{\text{th}} = v_{\text{th}}\tau = \sqrt{T/M}/\gamma$, where $v_{\text{th}} = \sqrt{T/M}$ is the thermal velocity and $\tau = M/\gamma$ is the typical relaxation time. Suppose a Brownian particle moves from a hot (T_1) to a cold (T_2) cell. When the particle crosses the border, it dissipates an amount of heat $(1/2)(T_1 - T_2)$ to the cold cell and then moves onward to the next hot cell or recrosses back to the same hot cell. As the overdamped limit ($M \rightarrow 0$) is approached, the thermal length scale goes to zero and the Brownian particle thermalizes more quickly to its new environment as it crosses a temperature boundary and thereby dissipates more heat in the same time period. The effective temperature gradient over which this thermalization of the kinetic energy occurs is $|T_1 - T_2|/l_{\text{th}} \propto M^{-1/2}$ and as $M \rightarrow 0$, this kinetic energy contribution diverges. Consequently, the entropy production also goes to infinity in the overdamped limit ($M \rightarrow 0$). Since this irreversible heat dominates the heat flow via potential, the efficiency diminishes to zero as \sqrt{M} , in the overdamped limit.

On the other hand, in the underdamped limit ($M \rightarrow \infty$), the Brownian particle doesn't thermalize to the local environment before entering the next heat bath [32] and the motor fails, diminishing the power and efficiency to zero. The efficiency will be maximum at an optimal value of M . Figure 4, clearly confirms these predictions. Simulations were also carried out for same friction coefficients in both the hot and cold baths, but the qualitative dependence on the mass of the Brownian particle remains the same.

IV. PERFORMANCE OF HEAT PUMP

We now discuss the energetics of the BL heat pump. When the external load exceeds the stall load, Brownian particles reverse their direction to move in the same direction as F . Overdamped models [11, 12, 17] predict that for $F > F_{\text{stall}}$ Brownian particles will transfer heat against the temperature gradient, from the cold to the hot bath, functioning as a heat pump and at the stalled state the coefficient of performance ε will attain the Carnot coefficient of performance ε_c .

In Fig. 5, we plot the total power input (\dot{W}), various heat flows out of the hot and cold cells as a function of the external load including the entropy production and the coefficient of performance of the heat pump. In contradiction to results obtained using overdamped models [11, 12, 17], we observe that the stalled state at which the current changes its direction is not the transition point from the heat engine to the heat pump. At the stalled state, the heat flow via potential, which fol-

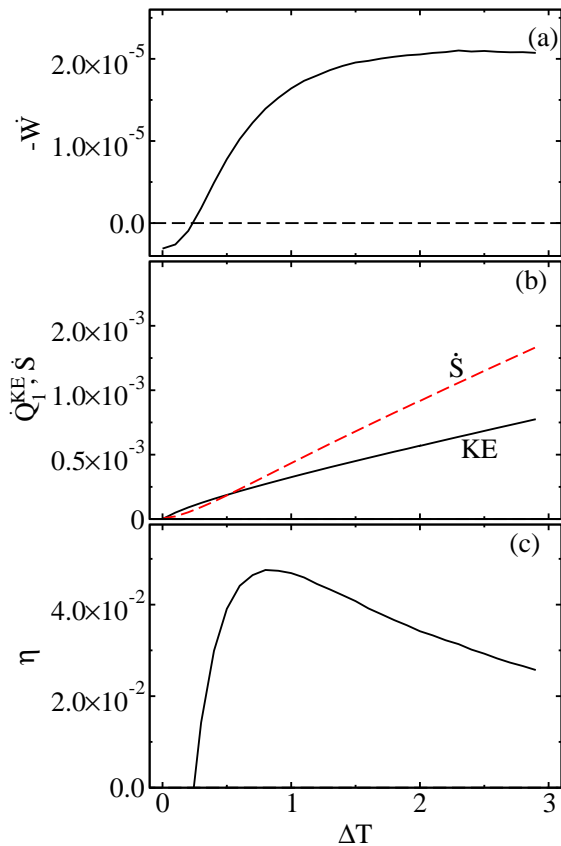


FIG. 3: (a) Power output, (b) heat flux due to kinetic energy and the entropy production (\dot{S}) and (c) efficiency as a function of $\Delta T = T_1 - T_2$, where T_2 is kept at 0.1. The parameter values are $M/m = 5.0$, $|F|L/2U_0 = 0.5$ and $\sigma_B = 5.0$. In (a), the thin horizontal dashed line represents $y = 0$. The Carnot efficiency varies from 0.67 at $\Delta T = 0.2$ to 0.96 at $\Delta T = 2.8$.

lowers the direction of the particle flux $\langle v \rangle$, goes to zero. However, there is still a net heat transfer from the hot to the cold cell due to the kinetic energy contribution. In fact, the heat flow via kinetic energy never vanishes and always flows from the hot to the cold reservoir regardless of the direction of particle current and magnitude of the external load. The positivity of the entropy production at all values of the external force also illustrates the validity of the second law for our system.

Figure 5 shows that starting from the stall load there is a region where the model works neither as a heat engine nor as a heat pump i.e., heat flows from the hot to the cold cell while work is being done on the Brownian particle. Refrigeration starts only when the heat flow via potential exceeds the sum of joule heat dissipated to the cold bath and the heat transfer via kinetic energy. As the external force is further enhanced, the joule heat (varying as $|F|^2$), which originates from the power input \dot{W} and the frictional force in case of the heat pump, eventually dominates the heat flow via potential (varying as $|F|$) and the cooling stops at a certain large value of F .

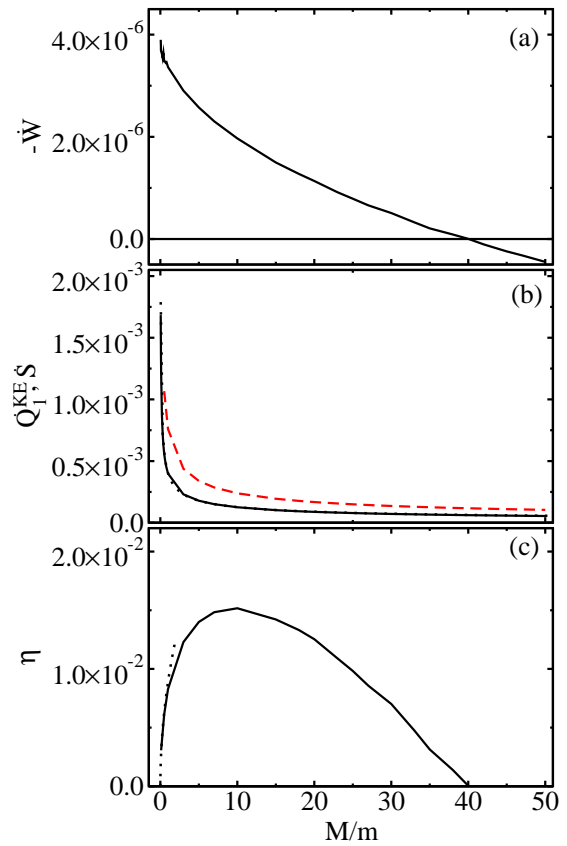


FIG. 4: (a) Power output, (b) heat flux due to kinetic energy (solid line) and entropy production \dot{S} (dashed line) and, (c) efficiency as a function of the mass ratio M/m . The dotted line in (b) corresponds to a phenomenological fit ($\propto M^{-1/2}$) to the kinetic energy contribution. The dotted line in (c) represents a fit ($\propto \sqrt{M}$) to the efficiency in the overdamped limit ($M \rightarrow 0$). In (a), the thin horizontal solid line represents $y = 0$. The parameter values are $T_1 = 0.7$, $T_2 = 0.3$, $|F|L/2U_0 = 0.3$ and $\sigma_B = 5.0$. The Carnot efficiency $\eta_c = 0.57$.

Beyond this value of the external force, \dot{Q}_2 is negative showing that net heat is also dissipated to the cold bath. The negative value for the coefficient of performance correspond to this situation, where the refrigeration fails. There is an optimal load at which the heat flow out of the cold cell and the coefficient of performance attain a maximum but ε is far below ε_c , due to the irreversible heat flow via kinetic energy.

In Fig. 6, we show the various thermodynamic quantities as a function of the temperature difference between the cells. We keep T_2 constant and vary T_1 . As the temperature difference between the baths increases, the net negative current in the direction of F will decrease as the increasing temperature of the hot bath will try to drive the Brownian particle in the forward direction. This decreases the heat flow via potential, which is proportional to the current, and hence the heat pump's abil-

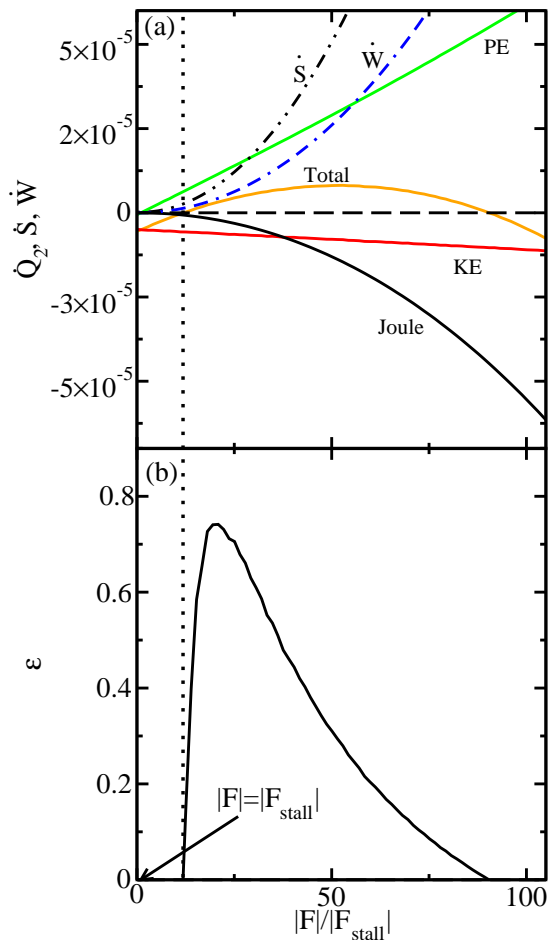


FIG. 5: (a) Power input \dot{W} (blue double dash-dotted line), various components of \dot{Q}_2 [from top to bottom the heat flows are \dot{Q}_2^{PE} (green line), \dot{Q}_2 (orange line), \dot{Q}_2^{KE} (red line) and \dot{Q}_2^{J} (black line)], the entropy production \dot{S} (black dash double dotted line) and (b) the coefficient of performance ε as a function of F/F_{stall} , F_{stall} being the stall load. In (a), the thin horizontal dashed line represents $y = 0$. The vertical line coincides with the value for the load where the cooling begins i.e. $|\dot{Q}_2^{\text{PE}}| > |\dot{Q}_2^{\text{KE}}| + |\dot{Q}_2^{\text{J}}|$. The parameter values are $\Delta T = T_1 - T_2 = 0.01$, $T_2 = 0.5$, $M/m = 5.0$ and $\sigma_B = 5.0$. The Carnot coefficient of performance $\varepsilon_c = 50$.

ity to transfer heat against the thermal gradient. The joule heat also decreases with ΔT . However, as $\Delta T \ll 1$, this decrease is marginal. On the other hand, the irreversible heat dumped to the cold cell via kinetic energy, increases significantly with ΔT and greatly reduces the cooling. In fact, beyond a small temperature difference $\Delta T \ll 1$, refrigeration fails, as Fig. 6 shows. The coefficient of performance is monotonically reduced with increasing temperature difference between the cells and is much smaller compared to the Carnot coefficient of performance due to the large entropy production.

In Fig. 7 we plot a phase diagram for our system in the $F - \Delta T$ plane. Clearly, the motor (heat engine) and

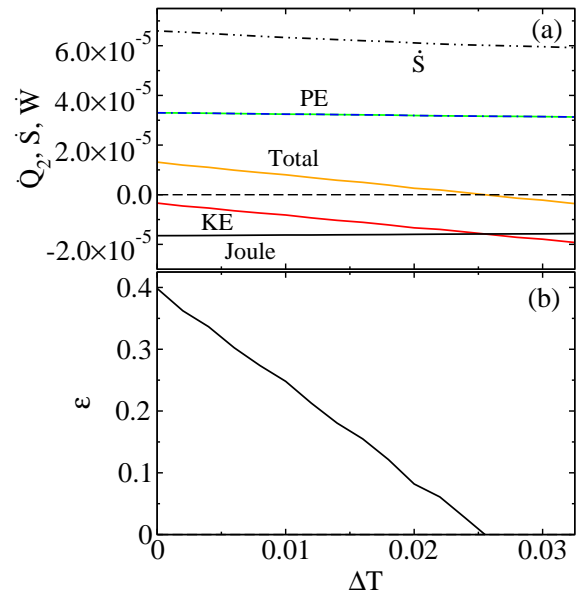


FIG. 6: (a) Power input \dot{W} (blue double dash-dotted line), various components of \dot{Q}_2 [from top to bottom the heat flows are \dot{Q}_2^{PE} (green line), \dot{Q}_2 (orange line), \dot{Q}_2^{KE} (red line) and \dot{Q}_2^{J} (black line)], the entropy production \dot{S} (black dash double dotted line) and, (b) the coefficient of performance ε as a function of ΔT for $M/m = 5.0$, $\sigma_B = 5.0$, $|F|L/2U_0 = 0.5$. \dot{W} and \dot{Q}_2^{PE} coincide because the external force F is half of the force due to the potential i.e. $-2U_0/L$. Eqs.(9) and (7) confirm this equality. In (a), the thin horizontal dashed line represents $y = 0$. Temperature of the cold bath is kept constant at $T_2 = 0.5$ and T_1 is varied. ε_c varies from ∞ at $\Delta T = 0$ to 20 at $\Delta T = 0.025$.

fridge (heat pump) regions do not touch each other (unlike overdamped models where the boundaries of the heat pump and heat engine regions touch [17, 33]) and there is a large region (white space) where the system works neither as a heat engine nor as a heat pump. This corresponds to the situation where a net heat is dissipated to the cold bath (due to the kinetic energy contribution or the joule heat) while the Brownian particles move in the direction of the external force.

V. LINEAR IRREVERSIBLE THERMODYNAMICS

In this section we discuss the efficiency and coefficient of performance of the BL system in the linear response regime. The BL heat engine and heat pump are a result of a cross effect between the external force F and the temperature difference $\Delta T = T_1 - T_2$. If they are small, there exists a linear relationship between the thermodynamic fluxes ($\langle v \rangle$ and $\dot{Q}_{1 \rightarrow 2}$) and thermodynamic forces

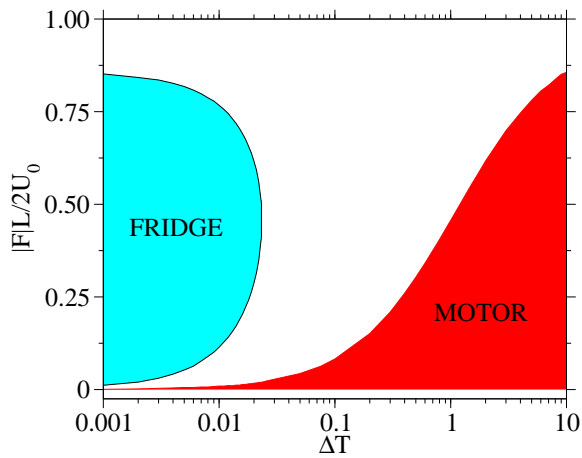


FIG. 7: The cyan and red areas represent the region where the system works as a fridge (heat pump) and motor (heat engine) respectively. The white area represents the region where the system acts neither as a heat engine nor as a heat pump. $M/m = 5.0$, $\sigma_B = 5.0$. ΔT is varied by keeping initially $T_1 = T_2 = 0.5$ and varying T_1 .

(F/T and $\Delta T/T^2$):

$$\begin{aligned} \langle v \rangle &= L_{11} \frac{F}{T} + L_{12} \frac{\Delta T}{T^2}, \\ \dot{Q}_{1 \rightarrow 2} &= L_{21} \frac{F}{T} + L_{22} \frac{\Delta T}{T^2}, \end{aligned} \quad (17)$$

where L_{ij} 's ($i, j = 1, 2$) are the Onsager transport coefficients, $T_1 = T + \Delta T/2$ and $T_2 = T - \Delta T/2$.

The efficiency of the heat engine is given by,

$$\eta = \frac{-\dot{W}}{\dot{Q}_{1 \rightarrow 2}} = \frac{-F \left(L_{11} \frac{F}{T} + L_{12} \frac{\Delta T}{T^2} \right)}{L_{21} \frac{F}{T} + L_{22} \frac{\Delta T}{T^2}}. \quad (18)$$

Recently, Van den Broeck [34] investigated the efficiency of Brownian heat engines in the linear response regime and concluded that, in principle, Carnot efficiency can be attained. He argued that for small F , the temperature difference ΔT drives the heat engine in the forward direction and simultaneously there is a heat transfer from the hot to the cold reservoir. As F increases, we ultimately reach the quasistatic condition of zero velocity at the stall load F_{stall} . From Eq. (17), we find that the stall load is given by,

$$F_{stall} = -\frac{L_{12}}{L_{11}} \left(\frac{\Delta T}{T} \right). \quad (19)$$

Beyond the stall load, the Brownian particles reverse their direction, transferring heat against the temperature gradient as a heat pump. In an ideal system, the velocity and heat reverse directions at the same value of F_{stall} so that $\langle v \rangle$ and $\dot{Q}_{1 \rightarrow 2}$ vanish for non-zero F and ΔT . Substituting the value of F_{stall} for F in Eq. (18), we find that this happens only when the condition of zero

entropy production: $L_{11}L_{22} = L_{12}L_{21}$ holds, and Onsager symmetry relationship is valid. This condition is referred to as ‘‘tight coupling’’ condition and when it is satisfied, we find that efficiency at the quasistatic limit is equal to the Carnot efficiency: $\Delta T/T$.

Carnot efficiency, however, can only be reached in the quasistatic condition where the velocity of the Brownian motor is zero, and hence it does not deliver any work. In practice a motor, must perform finite work in a finite time. A more practical measure of the motor efficiency is the efficiency when it delivers maximum power. Curzon and Ahlborn [19] claimed that the efficiency at maximum power η^* is bounded by the Curzon-Ahlborn efficiency, $\eta_{max}^* = 1 - \sqrt{T_2/T_1}$, where $T_1 > T_2$. The claim was found to be valid for thermal motors [18]. Using overdamped models, Asfaw and Bekele [11] studied the efficiency at maximum power (η^*) of the BL heat engine and found that η^* approaches η_{max}^* as the temperature difference between the reservoirs $T_1 - T_2 = \Delta T \rightarrow 0$. Apart from the fact that they used overdamped models, their definition of work was different from the thermodynamic definition. In order to evaluate efficiency at maximum power, we must use the proper thermodynamic definition of work (Eq. (9)) and since heat flow via kinetic energy is the dominant source of heat transfer for the BL system, one must also take into account the inertia of the Brownian particle.

Maximum power will be attained at a value of the load F^* given by [18],

$$F^* = -\frac{L_{12}}{L_{11}} \left(\frac{\Delta T}{2T} \right). \quad (20)$$

Substituting the value of F^* in Eq. (18), we find that the efficiency at maximum power is given by,

$$\eta_q^* = \frac{\Delta T}{2T} \frac{q^2}{2 - q^2}, \quad (21)$$

where,

$$q = \frac{L_{12}}{\sqrt{L_{11}L_{22}}}. \quad (22)$$

If the necessary condition of zero entropy production is satisfied, then $q = 1$ and to the lowest order of ΔT , the efficiency at maximum power approaches the efficiency of an endoreversible heat engine at maximum power viz., the Curzon-Ahlborn efficiency: $\eta_{max}^* = 1 - \sqrt{T_2/T_1} \sim \Delta T/2T$ [19]. However, in a previous work [14] it was shown that the product of the diagonal coefficients $L_{11}L_{22}$ diverges as $(M/m)^{-1/2}$, reflecting the divergence of the kinetic energy contribution. The off-diagonal coefficients however, did not show this singular behaviour. Consequently, we find $L_{11}L_{22} \gg L_{12}L_{21}$ for all values of M/m indicating large entropy production and very low efficiency. Hence the BL heat engine can never attain the Carnot efficiency or the Curzon-Ahlborn efficiency.

The coefficient of performance of the heat pump is given by,

$$\varepsilon = \frac{-\dot{Q}_{1 \rightarrow 2}}{\dot{W}} = \frac{-L_{21} \frac{F}{T} - L_{22} \frac{\Delta T}{T^2}}{F \left(L_{11} \frac{F}{T} + L_{12} \frac{\Delta T}{T^2} \right)} \quad (23)$$

By similar arguments as in the case of the heat engine, it is easy to show that the coefficient of performance reaches the Carnot coefficient of performance $T/\Delta T$ in the quasistatic limit, only if the necessary condition $L_{11}L_{22} = L_{12}L_{21}$ holds.

In the quasistatic limit, the heat pump does not transfer any heat and hence is practically useless. Since Carnot coefficient of performance is only possible in the quasistatic limit, it is not an effective measure of the heat pump performance from a practical point of view. A heat pump must transfer heat in a finite time and similar to the efficiency at maximum power for the motor we must find the coefficient of performance of the heat pump, under conditions of maximum heat transfer from the cold to the hot bath. Following Van den Broeck's work [18], regarding the efficiency at maximum power for the motor, some authors have investigated the coefficient of performance of the refrigerator at maximum $\dot{Q}_{1 \rightarrow 2}(\Delta T/T)$ [20]. This quantity is maximum at a temperature difference ΔT^* , given by

$$\Delta T^* = -\frac{L_{21}}{L_{22}} \frac{FT}{2}. \quad (24)$$

Substituting the value of ΔT^* in place of ΔT in Eq.(23), we find that up to the lowest order of ΔT , the coefficient of performance at maximum $\dot{Q}_{1 \rightarrow 2}(\Delta T/T)$, is given by

$$\varepsilon_q^* = \frac{q^2}{2 - q^2} \frac{T}{2\Delta T} = \frac{L_{21}/L_{11}}{|F| (2 - q^2)} \quad (25)$$

Analogous to the efficiency at maximum power, ε^* is equal to a factor that depends on q only, times half the Carnot coefficient of performance. If the necessary condition for attaining the Carnot coefficient of performance, namely $L_{11}L_{22} = L_{12}L_{21}$ holds, then $q = 1$ and ε^* attains a maximum ε_{max}^* given by,

$$\varepsilon_{max}^* = \frac{T}{2\Delta T} = \frac{L_{21}}{L_{11}} \frac{1}{2|F|} \quad (26)$$

However, for the BL refrigerator, $q = 1$ will never be attainable due to the kinetic energy contribution [14] and consequently ε_q^* will be less than ε_{max}^* .

These predictions of linear irreversible thermodynamics concerning η^* and ε^* have not been verified when temperature is spatially inhomogeneous. One of our objectives is to investigate the validity of linear irreversible finite time thermodynamics for the BL heat-engine and heat pump via numerical simulation of the inertial Langevin equation.

From Fig. 2 we find that the power output $-\dot{W}$ reaches a maximum at an optimum value of the load F^* . We evaluate the efficiency at F^* , which is the efficiency at maximum power, as a function of ΔT . In Fig. 8, we plot as a

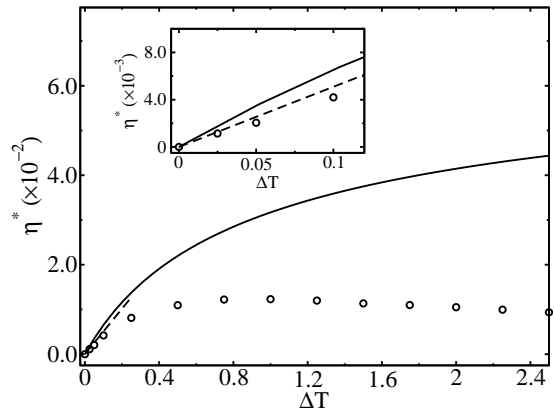


FIG. 8: η^* (symbols), η_q^* (dashed line) and the Curzon-Ahlborn efficiency η_{max}^* (solid line) as a function of $\Delta T = T_1 - T_2$, where the temperature of the cold cell is kept at $T_2 = 0.5$. η_{max}^* has been scaled ($\eta_{max}^* \times 0.075$) for easy visualization of all quantities on the same plot. The inset shows the detail of the efficiency at maximum power in the linear response regime. Parameter values are $M/m = 5.0$ and $\sigma_B = 0.5$.

function of ΔT , the Curzon-Ahlborn efficiency η_{max}^* , η^* obtained from numerical solution of the inertial Langevin equation and the efficiency at maximum power predicted by linear response theory, namely η_q^* . In order to determine η_q^* we have to find q , which was evaluated from the values of the Onsager coefficients, numerically. As the kinetic energy contribution is proportional to the temperature difference, it diminishes η^* to zero as $\Delta T \rightarrow \infty$, thus contradicting the results of Ref. [11], obtained using overdamped models. There is an optimum ΔT at which η^* reaches a weak maximum but it is far below η_{max}^* . In the linear response regime, there is good agreement between η^* and η_q^* , as shown in the inset of Fig. 8.

Performance of the refrigerator at maximum $\dot{Q}_{2 \rightarrow 1}\Delta T/T$ was also investigated numerically. The quantity $\dot{Q}_{2 \rightarrow 1}\Delta T/T$ reaches a maximum at an optimum value of the temperature difference, namely ΔT^* . We evaluated the coefficient of performance ε^* at ΔT^* as a function of $|F|$. Figure 9 shows that ε^* is always lower than ε_{max}^* due to the kinetic energy contribution. There is also good agreement between ε^* and the coefficient of performance predicted by linear response theory, ε_q^* .

VI. EFFICIENCY OPTIMIZATION

Figure 4 showed that $\eta(\varepsilon)$ reaches a maximum at optimum value of the mass between the overdamped and underdamped limits. In this regime, the efficiency can be further enhanced by reducing the kinetic energy contribution.

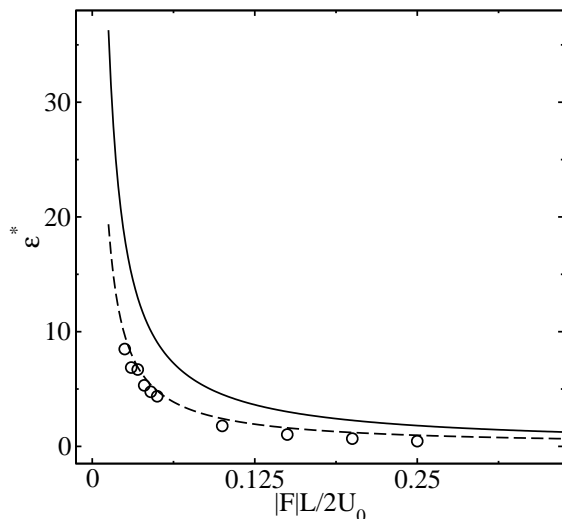


FIG. 9: ε^* obtained from numerical simulation (symbols), ε_q^* (dashed line) and ε_{max}^* (solid line), as a function of the external force. Parameter values are $M/m = 5.0$, $\sigma_B = 5.0$ and $T_1 = T_2 = 0.5$.

The main cause of the low efficiency and coefficient of performance in the BL heat engine and heat pump respectively is the heat transfer due to kinetic energy across the temperature boundary. When a temperature boundary coincides with the potential minima, the situation is the worst since the Brownian particle crosses the temperature boundary many times, resulting in a large heat transfer via kinetic energy. In order to reduce the number of crossings, we must move the temperature boundary away from the potential minima. On the other hand, the other temperature boundary should remain close to the potential maxima to maintain the current of Brownian particles.

Another way to minimize the number of crossings would be to keep the same temperature profile but modify the potential shape so that there is a small potential barrier of height $E < U_0$ at the location of the potential minima, which in our original model coincides with the temperature boundary. Since the Brownian particle is less likely to be found at a potential maxima, the number of crossings will decrease and consequently the kinetic energy contribution will be diminished.

Based on the above ideas, we will look for better models for the BL heat pump and heat engine by considering two approaches, one where we vary the temperature profile (*case I*) and the other where the potential shape (*case II*) is varied as compared to our original model.

While the efficiency reaches a maximum in between the overdamped and underdamped regimes, most microscopic systems can be described to a good approximation using overdamped dynamics. Moreover, most studies on the efficiency optimization of the BL heat engine and heat pump have been carried out in the overdamped regime

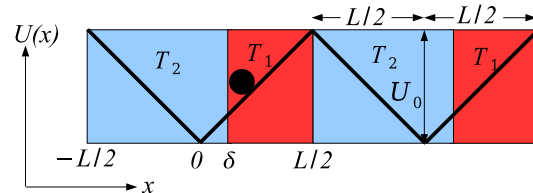


FIG. 10: (Color online) The temperature and potential profiles corresponding to *case I* of heat engine and heat pump. The dark circle represents the Brownian particle.

using overdamped models [10–12, 17, 25, 33]. However, as the overdamped model fails to predict the correct heat transfer we use the inertial Langevin equation [Eq. (2)] to study the efficiency optimization in the overdamped regime by choosing a large value for the friction coefficient, where good agreement is observed between the inertial Langevin equation and the overdamped model [14]. To this end, we carry out numerical simulations of Eq. (2) in the overdamped regime ($\gamma_{1,2} > 10.0$) with a dimensionless timestep $\tau = 0.0001$.

A. Heat Engine

In *case I*, we shift the location of the temperature boundary away from the potential minima. The potential $U(x)$ is the same as in our original model but the temperature profile $T(x)$ is modified and is now given by:

$$T(x) = \begin{cases} T_2 & \text{for } -\frac{L}{2} < x \leq \delta \\ T_1 & \text{for } \delta < x \leq L \end{cases} \quad (27)$$

where, $T_1 > T_2$ and the parameter δ specifies the location of the temperature boundary.

At $\delta/L = 0$, the cell boundary coincides with the potential maxima/minima and we go back to our previous model studied in section II. At $\delta/L = -1/2$ and $1/2$, the temperature becomes uniform since the width of the cold ($\delta/L = -1/2$)/hot ($\delta/L = 1/2$) cell goes to zero and the system ceases to work as a heat engine. The heat engine can deliver power for δ/L in the range $-1/2 < \delta/L < 1/2$. In Fig. 11, we plot the power output, heat flow and entropy production and efficiency as a function of the parameter δ/L . Figure 11 clearly shows that as the cell boundary moves away from the potential minima, in either direction, the irreversible heat transfer via kinetic energy and the entropy production decrease.

When $\delta/L > 0$, the presence of the cold region reduces the likelihood of the Brownian particle jumping over the barrier in the positive direction, especially if $(2U_0/L)\delta \gg T_2$, thus diminishing the current and the power $-\dot{W}$, and consequently the efficiency. On the other hand if δ/L is close to the potential minima, the kinetic

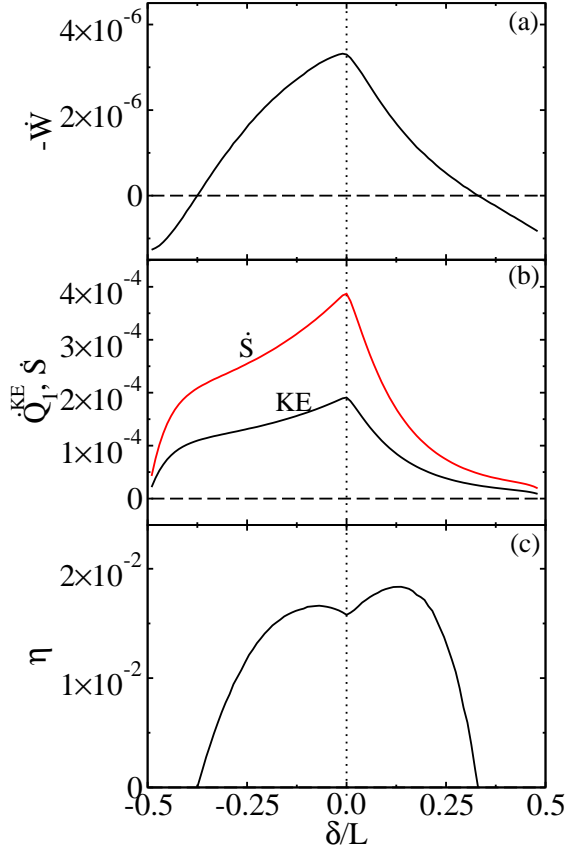


FIG. 11: (a) Power output ($-\dot{W}$), (b) entropy production and heat flux due to kinetic energy, and (c) efficiency as a function of δ/L for *case I* of heat engine, obtained from the inertial Langevin equation. In (a) and (b), the thin horizontal dashed line represents $y = 0$. Parameter values are $T_1 = 0.7$, $T_2 = 0.3$, $|F|L/2U_0 = 0.1$, $M/m = 5$ and $\sigma_B = 5.0$. The Carnot efficiency $\eta_c = 0.57$.

energy contribution becomes large, again reducing the efficiency. At an optimum $\delta/L > 0$, the efficiency is slightly maximized as shown in Fig. 11.

When $\delta/L < 0$, the hot region extends to the left of the potential minima at $x = 0$. This enhances the probability of the Brownian particle reaching the higher-potential-energy region and crossing the barrier in the negative direction. As a result, the net particle current in the positive direction and the power delivered by the Brownian particle diminish, thus reducing the efficiency. On the other hand, if δ/L is close to $x = 0$, the large heat transfer via kinetic energy reduces the efficiency. Figure 11 shows that there is an optimum $\delta/L < 0$, at which the efficiency is maximized. However, the maximum efficiency is far below the Carnot limit.

Now, we come to the second model. In *case II*, we keep the same temperature profile as in our original model [Eq. (4)] but change the potential profile $U(x)$, which is

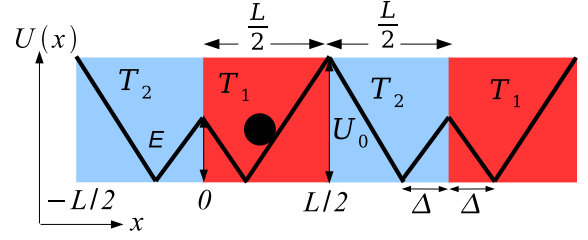


FIG. 12: (Color online) The temperature and potential profiles corresponding to *case II* of heat engine and heat pump. The dark circle represents the Brownian particle.

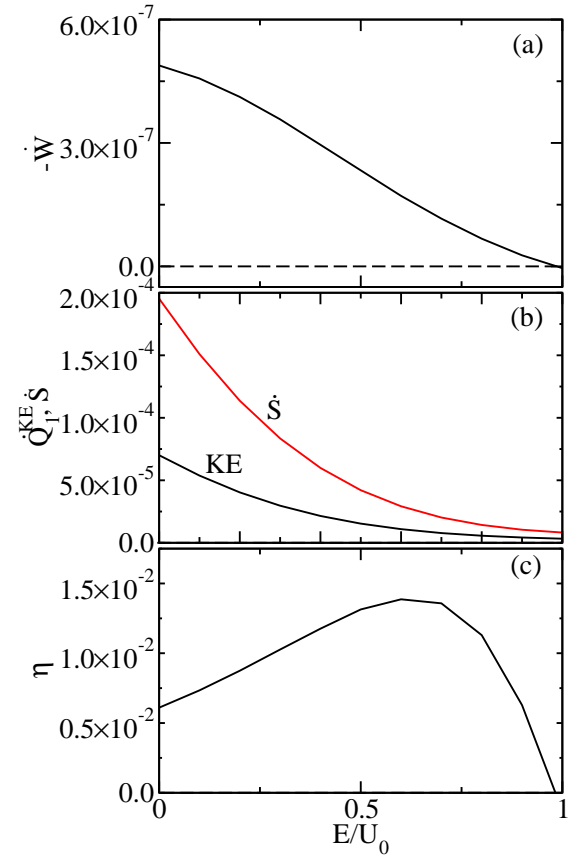


FIG. 13: (a) Power output, (b) entropy production and heat flux due to kinetic energy, and (c) efficiency as a function of E/U_0 for *case II* of heat engine. In (a), the thin horizontal dashed line represents $y = 0$. Parameter values are $T_1 = 0.4$, $T_2 = 0.2$, $\Delta/L = 0.1$, $|F|L/2U_0 = 0.025$, $M/m = 5$ and $\sigma_B = 5.0$. The Carnot efficiency $\eta_c = 0.5$.

now given by,

$$U(x) = \begin{cases} -\frac{2U_0}{L-2\Delta}(x + \Delta) & \text{for } -\frac{L}{2} < x \leq -\Delta \\ \frac{E}{\Delta}(x + \Delta) & \text{for } -\Delta < x \leq 0 \\ -\frac{E}{\Delta}(x - \Delta) & \text{for } 0 < x \leq \Delta \\ \frac{2U_0}{L-2\Delta}(x - \Delta) & \text{for } \Delta < x \leq \frac{L}{2} \end{cases} \quad (28)$$

Equation(28) shows that the potential has a barrier of height $E < U_0$ at $x = 0$, coinciding with the position of the potential minima in our original model.

In Fig. 13, we plot $-\dot{W}$, various components of \dot{Q}_1 and η as a function of the barrier height E at $x = 0$ normalized by U_0 . At $E/U_0 = 0$, the temperature boundary coincides with a potential minimum and the kinetic energy contribution is large thus leading to a low efficiency. As we increase E/U_0 , the irreversible heat transfer via kinetic energy as well as the net entropy production decreases as the recrossing of the Brownian particle near the temperature boundary at $x = 0$ is reduced on account of a potential maximum there. However, the motor velocity and consequently the power is diminished as well because the asymmetry around a potential minimum due to the inhomogeneous temperature decreases. The efficiency is maximized for $0 < E/U_0 < 1$, as shown in Fig. 13, though it remains far below the Carnot limit ($\eta_C = 0.5$).

B. Heat Pump

We now consider the performance of the BL heat pump corresponding to the same two cases, which were introduced in the previous subsection for the BL heat engine.

In Fig. 14, we plot the power input, heat flow out of cell 2, the entropy production and the coefficient of performance as a function of the location of the temperature boundary δ/L corresponding to *case I*. Since $\Delta T \ll 1$, the thermal gradient has a negligible effect on the particle current. Instead, the magnitude of the negative current is determined mostly by the potential shape and the external force F . However, the potential profile stays the same regardless of the position of the temperature boundary. Hence, the power input varies slowly with δ/L , as shown in Fig. 14.

As expected, Fig. 14 shows that the kinetic energy contribution and the entropy production become smaller as the temperature boundary is shifted away from the potential minima. The joule heat dissipated to the cold cell vanishes at $\delta/L = -1/2$ since the width of the cold region goes to zero at that point. As δ/L shifts to the right of $x = -1/2$, the joule heat starts to increase as the width of the cold cell becomes larger and reaches a maximum at $\delta/L = 1/2$, when the cold cell occupies the entire period L of the potential. As the temperature boundary is shifted to the left of $\delta/L = 0$, the heat flow via potential \dot{Q}_2^{PE} , is reduced since the width of the cold cell becomes smaller and less potential energy is extracted. When $\delta/L > 0$, \dot{Q}_2^{PE} again diminishes since the cold cell

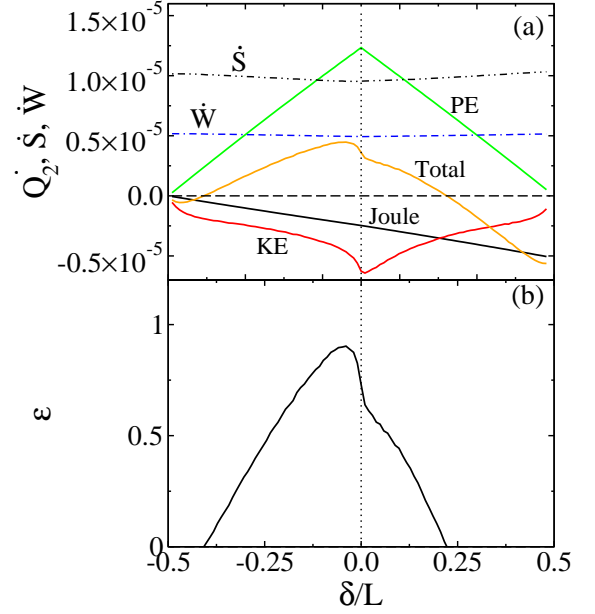


FIG. 14: (a) Power input \dot{W} , various components of \dot{Q}_2 (from top to bottom, the heat flows are \dot{Q}_2^{PE} , \dot{Q}_2 , \dot{Q}_2^{J} and \dot{Q}_2^{KE}) and entropy production and, (b) the coefficient of performance ε as a function of δ/L , corresponding to *case I* of heat pump, obtained from numerical solution of the inertial Langevin equation. In (a), the thin horizontal dashed line represents $y = 0$. The parameter values are $|F|L/2U_0 = 0.2$, $M/m = 5.0$ and $\sigma_B = 5.0$, $T_1 = 0.51$ and $T_2 = 0.5$. The Carnot coefficient of performance $\varepsilon_c = 50$.

now includes a portion of the negative slope as well. Figure 14 shows that there is an optimum $\delta/L < 0$ at which the total heat extracted from cell 2 and the coefficient of performance reach a maximum, showing that this model can enhance the cooling and refrigerator performance by appropriately changing the location of the temperature boundary. However, ε is still far below the Carnot coefficient of performance.

In *case II*, the small barrier at $x = 0$ reduces the heat transfer via kinetic energy and consequently the entropy. This is clearly seen in Fig. 15, Due to the small temperature difference, the current and consequently the power input and the joule heat vary slowly with E/U_0 . On the other hand, the barrier of height E at $x = 0$ diminishes the heat flow via potential because due to the negative slope, $-E/\Delta$, an amount of heat E is dissipated each time the Brownian particle crosses the cold cell, thus reducing the magnitude of potential energy extracted to $U_0 - E$. Since, heat flow via potential decreases with E/U_0 more rapidly as compared to the kinetic energy contribution, there is no optimum value of E/U_0 and net heat extracted from cell 2 decreases monotonically from a maximum at $E/U_0 = 0$. The coefficient of performance also decreases with E/U_0 and is far below ε_c . Hence, this case does not improve the performance of the refrigerator.

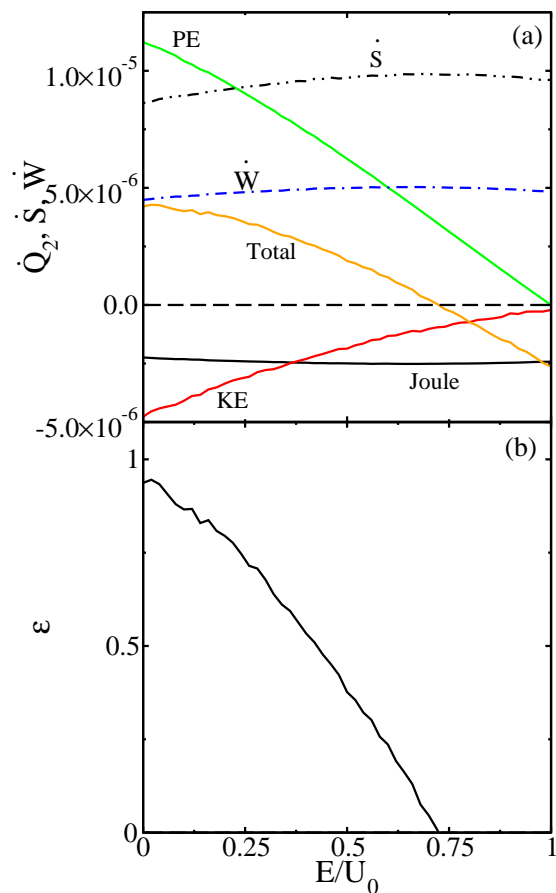


FIG. 15: (a) Power input \dot{W} , various components of \dot{Q}_2 (from top to bottom, the heat flows are \dot{Q}_2^{PE} , \dot{Q}_2 , \dot{Q}_2^{J} and \dot{Q}_2^{KE}) and entropy production and, (b) the coefficient of performance ε as a function of E/U_0 , corresponding to *case II* of heat pump, obtained from the inertial Langevin equation. In (a), the thin horizontal dashed line represents $y = 0$. The parameter values are $|F|L/2U_0 = 0.2$, $M/m = 5.0$ and $\sigma_B = 5.0$, $T_1 = 0.51$ and $T_2 = 0.5$. The Carnot coefficient of performance $\varepsilon_c = 50$.

VII. CONCLUSION

We studied the efficiency and coefficient of performance of the Buttiker-Landauer motor and refrigerator by numerical simulation of the inertial Langevin equation. Our results show qualitatively different behaviour

of the heat transfer, efficiency and coefficient of performance as a function of various parameters as compared to previous works based on overdamped models or other phenomenological approaches.

There is an optimal value of the mass at which the efficiency reaches a maximum. However, it is far below the Carnot limits. While there exists an optimal temperature difference between the hot and cold baths at which the efficiency of the motor is maximized the refrigerator performs best only when the temperature difference is small. We also found that the efficiency at maximum power can never attain the Curzon-Ahlborn efficiency due to the irreversible heat flow via kinetic energy. Due to this irreversible heat, the coefficient of performance of the refrigerator is below the theoretical maximum predicted by linear response theory, under conditions which could be considered as the equivalent of maximum power. The predictions of linear irreversible thermodynamics are in good agreement with numerical data. For the models we have studied, changing potential shape or the temperature profile in order to reduce the heat flow via kinetic energy reduces the particle current as well, leading only to a small enhancement of the motor efficiency and refrigerator coefficient of performance. We have performed numerical simulations of a few other models introduced by other authors in the context of efficiency optimization but in all cases decrease of kinetic energy also reduced the power output and the gain in efficiency was negligible.

From our results it is observed that reduction of heat transfer via kinetic energy also leads to a diminishing of the particle current thus making the motor marginally more efficient. In a recent work, Berger *et al.* [35] followed another approach where they optimized the potential to maximize the power output for a piecewise linear temperature profile. In fact the optimal potential obtained by them led to a diverging particle current in the overdamped limit. However, it is not clear whether such a potential will also lead to a reduction of the irreversible heat via kinetic energy and thus to a higher efficiency.

The next question to address is how one can reduce the irreversible heat without decreasing the particle current. At a more fundamental level, it would be interesting to obtain theoretically the maximum efficiency at maximum power and the equivalent maximum for the coefficient of performance. Answering such questions would also enhance our understanding of non-equilibrium thermodynamics at the small scale.

[1] R. Landauer, J. Stat. Phys. **53**, 233 (1988).
[2] N. G. Van Kampen, IBM J. Res. Develop, **32**, 107 (1988).
[3] N. G. Van Kampen, J. Stat. Phys., **63**, 1019 (1991).
[4] M. Büttiker, Z. Phys. B **68**, 161 (1987).
[5] R. P. Feynman, R. B. Leighton, and M. Sands, *The Feynman Lectures on Physics* (Addison Wesley, Reading, MA, 1966), Vol. I, Chap. 46.
[6] P. Reimann, Phys. Rep. **361**, 57 (2002).

[7] M. Bier and R. D. Astumian, Bioelectrochem. Bioenerg., **39**, 67 (1996).
[8] I. Derényi and R. D. Astumian, Phys. Rev. E **59**, R6219 (1999).
[9] T. Hondou and K. Sekimoto, Phys. Rev. E **62**, 6021 (2000).
[10] M. Matsuo and S. -I. Sasa, Physica A **276**, 188 (2000).
[11] M. Asfaw and M. Bekele, Eur. Phys. J. B **38**, 457 (2004).

- [12] B. -Q. Ai, H. -Z. Xie, D. -H. Wen, X. -M. Liu, and L. -G. Liu, *Eur. Phys. J. B* **48**, 101 (2005); B. -Q. Ai, L. Wang, and L. -G. Liu, *Phys. Lett. A* **352**, 286 (2006).
- [13] H. Goko, *J. Phys. Soc. Jpn.* **74**, 2453 (2005).
- [14] R. Benjamin and R. Kawai, *Phys. Rev. E* **77**, 051132 (2008).
- [15] J. M. R. Parrondo and B. J. de Cisneros, *Appl. Phys. A: Mater. Sci. Process.* **75**, 179 (2002)
- [16] K. Sekimoto, *J. Phys. Soc. Jpn.* **66**, 1234 (1997).
- [17] M. Asfaw and M. Bekele, *Physica A* **384**, 346 (2007).
- [18] C. Van den Broeck, *Phys. Rev. Lett.* **95**, 1 (2005).
- [19] F. L. Curzon and B. Ahlborn, *Am. J. Phys.* **43**, 22 (1975).
- [20] B. Jimenez de Cisneros, L. A. Arias-Hernandez and A. C. Hernandez, *Phys. Rev. E* **73**, 057103 (2006).
- [21] Y. Izumida and K. Okuda, *Eur. Phys. Lett.* **77**, 499 (2010).
- [22] Y. Izumida and K. Okuda, *Eur. Phys. Lett.* **97**, 10004 (2012).
- [23] Z. C. Tu, *J. Phys. A: Math. Theor.* **41**, 312003 (2008).
- [24] A. Gomez-Marin and J. M. Sancho **74**, 062102 (2006).
- [25] M. Asfaw, *Eur. Phys. J. B* **65**, 109 (2008).
- [26] Y. Zhang, J. He and Y. Xiao **28**, 100506 (2011).
- [27] B. Lin and J. Chen, *J. Phys. A: Math. Theor.* **42**, 075006 (2009).
- [28] P. Meurs, C. Van den Broeck, and A. Garcia, *Phys. Rev. E* **70**, 051109 (2004).
- [29] Peter. E. Kloeden and E. Platen, *Numerical Solution of Stochastic Differential Equations (Stochastic Modelling and Applied Probability)*. Springer, New York, 2000.
- [30] K. Sekimoto, *Prog. Theor. Phys. Suppl.* **130**, 17 (1998).
- [31] K. Sekimoto, *Stochastic Energetics* (Springer, in preparation).
- [32] Y. M. Blanter and M. Büttiker, *Phys. Rev. Lett.* **81**, 4040 (1998).
- [33] M. Asfaw, *Eur. Phys. J B* **86**, 189 (2013).
- [34] C. Van den Broeck, *Adv. Chem. Phys.* **135**, 189 (2007).
- [35] F. Berger, T. Schmiedl, and U. Seifert, *Phys. Rev. E* **79**, 031118 (2009).